HHS Public Access

Author manuscript

J Mol Cell Cardiol. Author manuscript; available in PMC 2016 August 01.

Published in final edited form as:

J Mol Cell Cardiol. 2015 August ; 85: 104–116. doi:10.1016/j.yjmcc.2015.05.012.

Antioxidant treatment normalizes mitochondrial energetics and myocardial insulin sensitivity independently of changes in systemic metabolic homeostasis in a mouse model of the metabolic syndrome

Olesya Ilkun[1], **Nicole Wilde**[1], **Joseph Tunei**[1], **Karla M.P. Pires**[1], **Yi Zhu**[1,4], **Heiko Bugger**[1,5], **Jamie Soto**[1,2], **Benjamin Wayment**[3], **Curtis Olsen**[3], **Sheldon E. Litwin**[3,6], and **E. Dale Abel**[1,2]

[1]Division of Endocrinology, Metabolism, and Diabetes, Program in Molecular Medicine, University of Utah School of Medicine, Salt Lake City, UT, 84112

[2]Fraternal Order of Eagles Diabetes Research Center and Division of Endocrinology and Metabolism, Roy J. and Lucille A. Carver College of Medicine, University of Iowa, Iowa City, IA, 52242

[3]Division of Cardiology, University of Utah School of Medicine, Salt Lake City, UT

Abstract

Cardiac dysfunction in obesity is associated with mitochondrial dysfunction, oxidative stress and altered insulin sensitivity. Whether oxidative stress directly contributes to myocardial insulin resistance remains to be determined. This study tested the hypothesis that ROS scavenging will improve mitochondrial function and insulin sensitivity in the hearts of rodent models with varying degrees of insulin resistance and hyperglycemia. The catalytic antioxidant MnTBAP was administered to the uncoupling protein-diphtheria toxin A (UCP-DTA) mouse model of insulin resistance (IR) and obesity, at early and late time points in the evolution of IR, and to db/db mice with severe obesity and type-two diabetes. Mitochondrial function was measured in saponin-permeabilized cardiac fibers. Aconitase activity and hydrogen peroxide emission were measured in isolated mitochondria. Insulin-stimulated glucose oxidation, glycolysis and fatty acid oxidation rates were measured in isolated working hearts, and 2-deoxyglucose uptake was measured in isolated cardiomyocytes. Four weeks of MnTBAP attenuated glucose intolerance in 13-week-old UCP-DTA mice but was without effect in 24-week-old UCP-DTA mice and in db/db mice.

Corresponding author: E. Dale Abel MD PhD, Fraternal Order of Eagles Diabetes Research Center, Division of Endocrinology and Metabolism, Roy J. and Lucille A. Carver College of Medicine, University of Iowa, 4312 PBDB, 169 Newton Road, Iowa City, IA 52242, USA. DRCAdmin@uiowa.edu, Phone number: 319-353-3050, Fax number: 319-335-8327.

[4]Current Addresses:
Touchstone Diabetes Center, University of Texas, Southwestern, Dallas TX, USA.

[5]Heart Center, Cardiology and Angiology I, Freiburg University, Freiburg, Germany

[6]Division of Cardiology, Medical University of South Carolina, Charleston, SC, USA

Disclosure statement

All authors have no conflicts of interest to declare.

Appendix A. Supplementary data.

Despite the absence of improvement in the systemic metabolic milieu, MnTBAP reversed cardiac mitochondrial oxidative stress and improved mitochondrial bioenergetics by increasing ATP generation and reducing mitochondrial uncoupling in all models. MnTBAP also improved myocardial insulin mediated glucose metabolism in 13 and 24-week-old UCP-DTA mice. Pharmacological ROS scavenging improves myocardial energy metabolism and insulin responsiveness in obesity and type 2 diabetes via direct effects that might be independent of changes in systemic metabolism.

1. Introduction

Type-two diabetes and the metabolic syndrome more than double the risk for cardiovascular disease (CVD), a leading cause of death in middle- and high income countries. [1]. Therapeutic strategies based on lowering circulating glucose levels, have not reversed major cardiovascular complications in multiple clinical trials [2, 3], emphasizing that organ-specific mechanisms may play a significant role in the pathogenesis of CVD in insulin resistant subjects. The cardiomyocyte-specific changes may include decreased insulin-stimulated glucose uptake and utilization, mitochondrial dysfunction, and oxidative stress. Several lines of evidence suggest that insulin resistance is associated with mitochondrial abnormalities in the heart. Earlier studies in animal models have shown that in the hearts of diabetic and obese db/db and ob/ob mice, insulin resistance was observed together with impaired mitochondrial function, and increased production of reactive oxygen species (ROS) [4–6]. Consistent with these observations, genetic disruption of insulin signaling and insulin-stimulated glucose utilization in cardiomyocytes, promotes oxidative stress and mitochondrial dysfunction [7, 8]. *In vitro*, TNFα, dexamethasone or palmitate treatments impaired insulin-stimulated glucose transport and induced oxidative stress in cultured 3T3-L1 adipocytes or L6 myotubes [9, 10].

Although oxidative stress and mitochondrial dysfunction accompany the insulin resistant cardiac phenotype, it is incompletely understood whether insulin resistance is primary or secondary to oxidative stress or mitochondrial dysfunction in the heart. This study was designed to test the hypothesis that myocardial insulin-resistance in obesity is secondary to mitochondrial dysfunction and increased oxidative stress. If true, then treatment with a mitochondria-targeted antioxidant might restore mitochondrial function and improve myocardial insulin sensitivity. To test this hypothesis, we used several mouse models of mild to severe hyperglycemia and obesity, namely UCP-DTA and db/db mice [5, 11]. UCP-DTA mice have a defect in peripheral energy expenditure and develop obesity on normal chow diet. Their pathophysiology has been extensively studied and parallel many of the metabolic abnormalities that are seen in animals fed a high-fat diet [12]. Moreover, the fatty acid composition of certain high-fat diets might have independent mitochondrial effects, which could confound the mitochondrial phenotype [13–15]. db/db mice were chosen to model extreme insulin resistance, obesity and diabetes. Importantly, both of these models have been previously characterized and shown to have impaired myocardial mitochondrial ATP synthesis [5, 11].

In addition to being the primary source of energy in the heart, mitochondria are an important source of superoxide that may contribute to oxidative stress. Therefore, we chose to pharmacologically inhibit ROS in the heart by utilizing catalytic activity of the mitochondrial antioxidant Mn (III) tetrakis (4-benzoic acid) porphyrin (MnTBAP), an established pharmacological scavenger of superoxide, whose mitochondrial superoxide dismutase (SOD2 or MnSOD) and catalase activity helps to detoxify superoxide to water [16, 17]. Treatment of ob/ob mice with MnTBAP increased glucose tolerance in the fed state [10], and glucose disposal into muscle and fat in high fat-fed mice [9]. *In vitro*, MnTBAP also restored GLUT4 translocation in insulin resistant L6 myotubes [9].

In the present study we show that systemic administration of MnTBAP reduced cardiac oxidative stress and improved mitochondrial function and myocardial insulin sensitivity in UCP-DTA mice and normalized myocardial mitochondrial dysfunction and fatty acid utilization in db/db mice independent of changes in systemic metabolic homeostasis. Thus, in independent murine models that span the spectrum of obesity and insulin resistance, we provide evidence that targeted antioxidants might act directly to restore mitochondrial bioenergetics and insulin sensitivity in the heart.

2. Methods

2.1. Animals

Protocols for animal care and experimentation were approved by the Institutional Animal Care and Use Committee of the University of Utah. UCP-DTA and littermate control mice (WT) were bred and maintained at the University of Utah until the ages of 13 or 24 weeks. UCP-DTA mice are on the FVB genetic background. Db/db mice and their WT controls were obtained from The Jackson Laboratory and maintained until 9 weeks of age. Db/db mice are on the C57BL/6J genetic background. All mice were kept in temperature-controlled animal facilities (21–23°C) on 12h light (6:00AM – 6:00PM) and 12h dark cycle and fed standard chow diet (#8656 Harlan Teklad, Madison, WI) *ad libitum*. MnTBAP [Mn (III) tetrakis (4-benzoic acid) porphyrin chloride solution in alkalized saline (VWR, PA) was administered intraperitoneally to UCP-DTA and wildtype littermate controls (WT) at 20mg/kg, 3 times/week for 4 weeks starting at the age of 9 or 20 weeks. For db/db mice, MnTBAP was administered 3 times/week for 3–4 weeks starting at the age of 6 weeks.

2.2. Body composition

Mice were sedated with an intraperitoneal injection of chloral hydrate (0.03 mg/g of body weight). Dual Energy X-ray Absorptiometry (DEXA) scans were performed using the Norland pDEXA™ (Trumbull, CT) scanner. In 13 week-old UCP-DTA mice, epididymal and retroperitoneal white adipose tissue was removed and individually weighed.

2.3. Glucose tolerance test

13 and 24 week-old UCP-DTA and 9 week-old db/db mice and respective controls were fasted for 6 hours, and glucose tolerance tests were performed as previously described [18]. Briefly, basal blood glucose levels were measured after a 6-hour fast using a standard glucometer (Bayer, IN). Glucose was dissolved in 0.9% saline (1mg/g body weight) and

administered as a single intraperitoneal injection. Blood glucose was measured right before the injection and 5, 15, 30, 60, and 120 minutes after the injection using the same glucometer.

2.4. Mitochondrial isolation

Cardiac ventricles were cleaned of blood and minced in STE1 buffer (on ice), and homogenized in a Potter-Elvejhem glass homogenizer. Mitochondria were isolated using a series of differential centrifugations as previously described [7].

2.5. Hydrogen peroxide emission by isolated mitochondria

An increase in the fluorescence of oxidized homovanillic acid by H_2O_2 emitted by the isolated mitochondria was measured as previously described [5]. Briefly, an increase in fluorescence (Ex. 312 nm, Em. 420nm) was monitored after addition of oligomycin (1ug/mL) and succinate (4 mM) to isolated cardiac mitochondria. The contribution of complex I to ROS production was assessed following the addition of the complex I inhibitor, rotenone (4 uM).

2.6. Aconitase activity assay

Activity of mitochondrial aconitase was measured in isolated mitochondria as previously described [19].

2.7. Mitochondrial oxygen consumption and ATP production

Mitochondrial respiration rate and ATP synthesis rate were measured as previously described [4, 5]. Briefly, basal, ADP-stimulated, oligomycin-inhibited mitochondrial respiration was measured in saponin-permeabilized fibers from left ventricle, using palmitoyl-carnitine (0.02 mM) and malate (2 mM) or glutamate (5mM) and malate (2 mM) as substrates. ATP production was measured in ADP-stimulated samples using the Enliten Luciferase/Luciferin Reagent (Promega, Madison, WI). In addition, db/db hearts were perfused with palmitate (1 mM) and glucose (11 mM) in the Langendorff mode prior to fiber separation and measurement of mitochondrial respiration [5].

2.8. Electron microscopy and stereology

Hearts were removed and 1x1x1 mm cubes excised from left ventricular endocardium and subendocardium, and placed in standard fixative (1% paraformaldehyde, 2.5% glutaraldehyde, 0.1 M sodium cacodylate, 2.4% sucrose and 8mM $CaCl_2$pH 7.4), processed, and analyzed as previously described [5]. Mitochondrial number and volume density were quantified using stereology.

2.9. Insulin stimulation of mice

Mice were fasted for 6 hours and anesthetized with 0.07 mg/g body weight I.P. chloral hydrate. 0.1 IU of human regular insulin or equal volume of saline was injected with via the inferior vena cava (IVC) as previously described [20]. Hearts were then harvested 5 minutes following injection, and frozen in liquid nitrogen. Cardiac perfusions in the Langendorff

mode were also applied to 13 week UCP-DTA using Krebs Henseleit buffer with and without 2nM insulin as previously described [21].

2.10. Glucose uptake by isolated cardiomyocytes

Cardiomyocytes were isolated from the perfused hearts and ^{3}H-2-deoxyglucose uptake was measured as previously described [22]. Briefly, hearts were perfused with collagenase-containing buffer, isolated cardiomyocytes were plated, deprived of glucose, and treated with 0, 0.1, 1, or 10 nM insulin for 40 minutes, followed by a 30 minute treatment with ^{3}H-2-deoxyglucose.

2.11. Substrate utilization, MVO_2, and cardiac function in isolated working hearts

Glycolysis, glucose and palmitate oxidation, MVO_2, and *ex vivo* cardiac function were measured in isolated working hearts of 13 and 24 week-old UCP-DTA and 9-week-old db/db mice and respective controls treated with MnTBAP or saline as previously reported [22, 23]. Briefly, to determine glycolysis and glucose oxidation rates, hearts were perfused with Krebs Henseleit buffer containing 0.4 mM palmitate, 5mM glucose (with addition of [5–^{3}H] glucose and [U-^{14}C] glucose as tracers) with or without 1 nM insulin. $^{3}H_2O$ and $^{14}CO_2$ released from heart perfusates are used to calculate the rates of glycolysis and glucose oxidation, respectively. To measure palmitate oxidation rate, a separate group of hearts was perfused with [9 –10-^{3}H] palmitate and the rate was calculated from released $^{3}H_2O$.

2.12. Western blot analysis

Hearts removed from mice following IVC injection of insulin or saline or following Langendorff perfusion were used to prepare protein extracts as previously described [24]. Proteins were resolved by SDS-PAGE, transferred to PVDF or nitrocellulose membranes and probed with corresponding primary antibodies: phospho-Akt (Ser473), Akt, phospho-GSK-3β (Ser 9), GSK-3β (Santa Cruz Biotechnology, Santa Cruz, CA), NDUFA9 (OxPhos complex I), SDHB (OxPhos complex II), UQCRC1 (OxPhos complex III), F1complex, α-subunit (Oxphos complex V) (Molecular Probes-Invitrogen, Carlsbad, CA). Protein expression was detected and quantified using the Odyssey Infrared Imaging System and software (Lincoln, NE). Secondary antibodies: Alexa Fluor-conjugated anti-Rabbit 680, and anti-Mouse 680 (Invitrogen, Carlsbad, CA), anti-Rabbit 800, and anti-Mouse 800 (VWR International, West Chester, PA).

2.13. Plasma levels of triglycerides, free fatty acids, insulin

Mice were fasted for 6 hours, and plasma samples were collected to determine concentrations of triglyceride (TG) and insulin as previously described [25].

2.14. Myocardial triglyceride content

Triglyceride levels were measured in frozen hearts as previously described [26]. Briefly, a chloroform / methanol mix (8:1 v/v) was used to extract lipids from heart homogenates. 3 hours later, H_2SO_4 was added to the mix, and the lipid layer was extracted, harvested, and

dried. Triglyceride and free glycerol reagents were used to quantify triglyceride in samples, and glycerol was used as a standard for quantifications (Sigma, St. Louis, MO).

2.15. Histology and stereology

Hearts were fixed with 10% zinc-formalin (Thermo Fisher Scientific, Waltham, MA) as previously described [27]. Sections were stained with hematoxylin-eosin or Masson's trichrome stains. Imaging was performed using an Olympus LX81 inverted light microscope (New York, NY). Cardiomyocyte cross-sectional area and left ventricular thickness were quantified from images taken by an Olympus Microfire Digital Camera as described [28].

2.16. In vivo cardiac function

24 week-old UCP-DTA and WT mice treated with MnTBAP or saline were sedated with isoflurane and echocardiography was performed using a linear 13 mHz probe (Vivid V echocardiograph, GE Healthcare, Tampa, FL) as previously described [29].

2.17. Gene expression

mRNA isolation and quantification was performed as previously described [5]. Briefly, frozen hearts were used for mRNA isolation using TRIzol reagent (Invitrogen). Isolated mRNA was purified using the RNA midi kit (Qiagen, Valencia, CA), reverse transcribed, and quantified by qPCR using an ABI Prism 7900HT (Foster City, CA). SYBR Green I and ROX dye (Invitrogen) were used as the internal reference. Expression of each gene was measured in triplicate (384-well plate format) and normalized to 16S ribosome transcript levels.

2.18. Statistical analysis

Data are expressed as mean ± standard error. Statistical analysis of data was performed using ANOVA and significance ($p<0.05$) was assessed using the post-hoc Fisher's protected least significant difference test with Statview 5.0.1 software (SAS Institute, Cary, NC).

3. Results

3.1. Metabolic parameters and body weight in UCP-DTA and db/db mice, treated with MnTBAP or saline

UCP-DTA, a mouse model of progressive obesity and insulin resistance, was created using uncoupling protein 1 (UCP1) to target a protein translation inhibitor, diphtheria toxin A (DTA), to brown adipocytes [30]. As a result, UCP-DTA mice have a marked reduction in UCP1 protein content and brown adipocyte mass, leading to reduced energy expenditure and gradual development of many manifestations of the metabolic syndrome such as obesity, hyperinsulinemia, and hyperlipidemia [11, 30].

Although there was a trend towards increased body weight in 13 week-old UCP-DTA mice relative to WT controls (Table 1), analysis of body composition by DEXA did not show differences in body composition between UCP-DTA and control mice following either MnTBAP or saline treatment (Figure 1A). We found however, that certain abdominal adipose tissue depots (measured as weight of perigonadal and perirenal fat pads) were

increased in saline-treated 13 week-old UCP-DTA mice and was normalized following MnTBAP treatment. MnTBAP did not affect abdominal adipose tissue content in control mice (Supplemental Figure 1).

24 week-old UCP-DTA mice weighed ~60% more than respective controls (Table 2). DEXA analysis of body composition revealed a significantly higher percentage fat mass and a proportionate reduction in lean mass ratio in UCP-DTA mice versus controls. Importantly, systemic administration of MnTBAP did not alter body composition (Figure 1B). In comparison, 9 week-old db/db mice had an ~80% increase in body weight, and MnTBAP treatment had no effect on body weight or weight gain in db/db mice relative to controls (Table 3).

13 and 24 week-old UCP-DTA mice had normal fasting glucose levels (Tables 1 and 2), but were glucose intolerant (Figure 1C, D). 9 week-old db/db mice were diabetic and had 2-fold higher fasting glucose levels. MnTBAP administration for 4 weeks significantly improved glucose tolerance in young UCP-DTA mice, but not in 24 week-old UCP-DTA mice or in db/db mice (Figure 1 C–E).

Compared to controls, UCP-DTA mice had ~2.5 fold increased fasting serum insulin concentrations by the age of 13 weeks, and almost 6-fold increase by the age of 24 weeks. In comparison, 9-week-old db/db mice had 9-fold higher insulin concentrations, and MnTBAP treatment did not alter these parameters (Table 3). Fasting serum triglyceride (TG) concentrations in saline-treated UCP-DTA mice were consistently ~1.5 fold higher relative to WT controls both at the age of 13 and 24 weeks. Interestingly, MnTBAP treatment lowered fasting levels of circulating TG in 13 but not 24 week-old UCP-DTA mice (Table 1 and 2). No reduction in fasting triglyceride levels was observed in MnTBAP-treated as compared to saline-treated db/db mice, however fed concentrations of TG were reduced by MnTBAP treatment of db/db mice (Table 3). Taken together, these data indicate that MnTBAP treatment may influence glucose tolerance and abdominal obesity only in the early stages in the evolution of insulin resistance and obesity, but may modulate circulating concentrations of TG.

3.2. MnTBAP attenuates cardiac hypertrophy in 24 week-old UCP-DTA mice

A trend towards increased heart weight was observed in 13 week-old UCP-DTA mice relative to WT controls and no effect of MnTBAP on cardiac growth was observed. In contrast, the heart weight of 24 week-old UCP-DTA mice was increased by ~30%. Interestingly, a significant reduction in heart weight was observed in 24 week-old MnTBAP-treated compared to saline-treated UCP-DTA mice (Table 2). These data were confirmed by histological analysis showing reduced cardiomyocyte cross sectional area relative to control hearts (Supplemental Figure 2). Echocardiographic analysis also confirmed a reduction in indices of ventricular hypertrophy (septal and posterior wall thickness and left ventricular internal diameter) in UCP-DTA mice treated with MnTBAP, relative to UCP-DTA mice treated with saline (Table 4). In *vivo* cardiac function was not impaired in 24 week-old UCP-DTA or control mice regardless of treatment. In contrast to cardiac hypertrophy observed in UCP-DTA mice, in db/db mice, compensated cardiac hypertrophy does not develop relative to the rapid expansion of body weight. In 9 week-old db/db mice, heart weight was not

different from controls, and MnTBAP treatment had no additional effect on cardiac growth (Table 3).

3.3. Oxidative stress in hearts of UCP-DTA mice

Mitochondrial reactive oxygen species are converted to H_2O_2 that may diffuse from the mitochondria. Therefore, H_2O_2 emission measures both mitochondrial ROS production and detoxification. Mitochondria from the hearts of 9 week-old db/db mice have increased H_2O_2 emission and other markers of oxidative stress [5]. We therefore sought to determine if similar changes were present in the UCP-DTA model. 13 week-old UCP-DTA mitochondria had a trend towards increased H_2O_2 emission relative to WT controls (Figure 2A). Another marker of mitochondrial oxidative stress, mitochondrial aconitase activity, was not significantly altered in 13 week-old UCP-DTA mice (Figure 2B). As animals aged, mitochondrial H_2O_2 emission was significantly increased and mitochondrial aconitase activity significantly reduced in saline-treated - 24 week-old UCP-DTA mice. MnTBAP treatment normalized these parameters (Figure 2C, D).

3.4. MnTBAP treatment improves mitochondrial function in UCP-DTA and db/db hearts

Permeabilized left ventricular fibers were used to measure mitochondrial function in UCP-DTA or db/db and control hearts. Mitochondrial respiration rates were normal in 13-week-old UCP-DTA mouse hearts, but ATP production rates and ATP/O ratios were reduced consistent with mitochondrial uncoupling. MnTBAP treatment restored mitochondrial coupling (Figure 3A, B). Of interest, MnTBAP treatment reduced ATP and ATP/O ratios in control hearts and reduced mitochondrial volume density in control and UCP-DTA hearts (Figure 3C). Cardiac mitochondria of 24 week-old UCP-DTA mice had impaired ADP-stimulated oxygen consumption in addition to mitochondrial uncoupling (Figure 4A). The abundance of OXPHOS subunits in complexes I (NDUFA9 subunit) and III (Core I subunit) were reduced in the hearts of saline- treated 24 week-old UCP-DTA mice and was reversed by MnTBAP treatment (Figure 4B). In contrast, reduced OXPHOS subunit composition was not evident in 13 week-old UCP-DTA mice (data not shown). The absence of any changes in expression of mRNAs encoding for these subunits (Supplemental Figure 3) suggests that post-translational mechanisms are responsible for altering the stoichiometry mitochondrial OXPHOS subunits. Similar to 13-week-old mice, MnTBAP treatment reduced mitochondrial volume density in 24-week-old WT and UCP-DTA mice (Figure 4C). Permeabilized fibers from db/db mice exhibited significant mitochondrial uncoupling characterized by reduced ATP production rates despite normal oxygen consumption rates (Figure 5 A–C). MnTBAP treatment partially restored mitochondrial ATP production and improved ATP/O ratios. Similar to observations in young UCP-DTA hearts, MnTBAP induced mitochondrial uncoupling in control hearts, but not the same degree as observed in saline-treated db/db hearts (Figure 5 B, C).

3.5. Impact of MnTBAP treatment on myocardial fatty acid utilization

To determine if altered myocardial substrate metabolism was associated with mitochondrial dysfunction in UCP-DTA and db/db hearts, we measured palmitate oxidation in isolated working hearts. There were no changes in palmitate oxidation in the hearts of 13- or 24-week-old UCP-DTA mice whether or not treated with MnTBAP (Figures 3D and 4D). In

contrast, db/db mice exhibited increased palmitate oxidation rates that were normalized following MnTBAP treatment (Figure 5D).

3.6. Insulin-stimulated myocardial glucose utilization is restored in MnTBAP-treated UCP-DTA hearts

Systemic insulin resistance in UCP-DTA mice is manifested by impaired glucose tolerance and hyperinsulinemia (Figure 1C, D). We therefore sought to determine if the regulation of myocardial glucose utilization by insulin was altered in UCP-DTA mice. Insulin-stimulated 2-deoxy-^{3}H-glucose (2-DG) accumulation was reduced in isolated cardiomyocytes from 13 and 24 week-old UCP-DTA hearts, and was normalized following MnTBAP treatment (Figure 6A, E).

In isolated working hearts, basal rates of glycolysis were reduced in 24-week-old UCP-DTA, but were normal at 13-weeks (Figure 6B, F). MnTBAP treatment normalized basal rates of glycolysis in 24-week-old UCP-DTA mouse hearts. There were no changes in basal rates of glucose oxidation. However insulin stimulated rates of glycolysis and glucose oxidation were significantly reduced in UCP-DTA mouse hearts of both ages and were normalized following MnTBAP treatment (Figure 6B, C, F, G). Basal glycolytic rates were reduced in saline-treated db/db mice relative to controls, but were restored following MnTBAP treatment. However, MnTBAP, did not normalize glucose oxidation rates in db/db hearts (Figure 6I, J)

Ex vivo cardiac power increased following insulin stimulation of 13 and 24 week-old saline- and MnTBAP-treated WT but not saline-treated UCP-DTA hearts (Figure 6D, H). Importantly, insulin-stimulated *ex vivo* cardiac power was significantly improved in 13 but not 24 week-old UCP-DTA hearts after systemic administration of MnTBAP (Figure 6D, H). There was no difference in basal cardiac power in db/db mice (Figure 6K).

3.7. Insulin signaling in UCP-DTA hearts

Insulin-stimulated phosphorylation of Akt at serine-473 was normal in 13 week-old UCP-DTA hearts (Figure 7A, B). Similarly, insulin-stimulated phosphorylation of Akt or its target GSK3 was essentially normal in the hearts of 24 week-old UCP-DTA mice (Figure 7C–E). Basal levels of phosphorylation of Akt and GSK3 in UCP-DTA were increased, potentially reflecting systemic hyperinsulinemia in these mice. If normalized to basal levels of Akt or GSK3 phosphorylation, the fold change in insulin stimulation was reduced in saline-treated UCP-DTA hearts, and restored with MnTBAP (Figure 7F, G).

4. Discussion

Mitochondria produce over 90% of the ATP required for normal cardiac function. Obesity and insulin resistance are associated with altered myocardial substrate metabolism and reduced mitochondrial function [5, 31]. This study investigated the impact of oxidative stress on the progression to mitochondrial dysfunction and myocardial insulin resistance in obese and insulin resistant UCP-DTA and db/db mice. In addition, we investigated whether mitochondrial targeted antioxidants could interrupt the cycle of increasing oxidative stress and worsening insulin resistance. Oxidative stress can occur because of increased generation

of reactive oxygen species (ROS) or their insufficient detoxification by antioxidant systems. Although several clinical trials have failed to show benefit of dietary administration of antioxidants, most of the substances tested might not have effectively reduced mitochondrial oxidative stress. A synthetic catalyst of superoxide detoxification, MnTBAP, was used in this study to scavenge mitochondrial ROS and to investigate the impact of oxidative stress on mitochondrial function and cardiomyocyte metabolism. In obese and insulin resistant UCP-DTA mice, MnTBAP treatment normalized aconitase activity and H_2O_2 emission by cardiac mitochondria.

Previous studies that have examined the role of mitochondria in obesity or diabetes-related mitochondrial dysfunction have used transgenic mouse models with overexpression of mitochondrial-targeted anti-oxidants [32, 33]. The impetus for our study was to determine if a pharmacological approach that targeted mitochondria would have similar effects. For this reason we used MnTBAP, which we and others have previously demonstrated will effectively scavenge mitochondrial ROS in the heart [18], as an initial proof of principle. Future studies with non-mitochondrial targeted antioxidants will be necessary to definitively prove that the mechanism of action is selective to mitochondria and does not involve cytosolic ROS overproduction.

Glucose intolerance and abdominal obesity was already evident in 13 week-old UCP-DTA mice. Here we show that early in the evolution of the metabolic syndrome, systemic MnTBAP administration significantly improved the metabolic milieu by normalizing glucose intolerance and hypertriglyceridemia in parallel with reduced visceral adiposity. By the age of 24 weeks, UCP-DTA exhibited a 30% increase of their body weight predominantly in the form of adipose tissue whereas control mice gained about 6%. An earlier study reported a partial improvement of glucose tolerance but not body weight in 20 week-old ob/ob mice daily treated with MnTBAP for 12 weeks [10]. Interestingly, the administration of MnTBAP for 4 weeks starting at 20 weeks of age did not affect glucose tolerance, body weight or body composition in UCP-DTA or control mice. We also found no effect of MnTBAP on body mass and glucose tolerance in obese and diabetic 9–10 week-old db/db mice after 3–4 weeks of MnTBAP treatment suggesting that the partial restoration of glucose tolerance in ob/ob mice reported by Houstis et al could be due to the much longer duration of MnTBAP treatment in those studies [10]. Although mitochondrial function in skeletal muscle might have been improved by short-term MnTBAP treatment, as we have previously reported in animal models of diet-induced obesity, it is not sufficient to improve systemic glucose homeostasis [34, 35]. Thus, given the higher energetic demand of cardiac mitochondria and potentially greater degrees of oxidative stress, the beneficial impact of MnTBAP on cardiac insulin signaling and glucose transport might be more readily discerned.

Since MnTBAP mimics the activity of the mitochondrial enzyme SOD2, the maximal effect of MnTBAP may be expected in a mitochondria-rich organ such as the heart as evidenced by improved mitochondrial function and insulin sensitivity in the hearts of UCP-DTA mice. The lack of significant whole-body effects of MnTBAP in 24 week-old mice is an important finding, because it raises the possibility that the beneficial effects of MnTBAP may reflect cardiac-specific effects, versus indirect effects arising from systemic actions. While

physiological levels of ROS may be important for normal cardiac development and function, oxidative stress may lead to cardiac hypertrophy by modulating multiple signaling pathways involved in stress responses [36, 37]. Mitochondrial ROS-induced oxidative stress has been linked to activation of pro-hypertrophic kinases and angiotensin II-induced cardiac hypertrophy [38–40]. 24 week-old UCP-DTA mice displayed compensated cardiomyocyte hypertrophy relative to age-matched controls, which was attenuated after 4 weeks of MnTBAP treatment, potentially by modulating hypertrophic signaling molecules by mitochondrial ROS.

MnTBAP treatment also significantly improved mitochondrial oxygen consumption, ATP synthesis and mitochondrial coupling in the hearts of 24 week-old UCP-DTA mice. MnTBAP restored the protein levels of representative subunits of mitochondrial OXPHOS complexes I and III in UCP-DTA hearts. These complexes are the main sites of mitochondrial ROS generation [41], and the damage to specific subunits or iron-sulfur clusters may make them susceptible to oxidative damage and degradation or improper assembly [42]. Reduced expression of mitochondrial OXPHOS complex I, mitochondrial dysfunction and overflow of ROS was previously documented in the hearts and skeletal muscle of insulin resistant and obese mice and humans, respectively [4, 43]. It is possible, that in the case of UCP-DTA mice, MnTBAP treatment reduced oxidative stress thereby eliminating a mechanism that potentially led to the reduction of OXPHOS complexes I and III.

We unexpectedly observed mitochondrial uncoupling and reduced ATP synthesis in MnTBAP-treated 9 or 13 week-old control mice regardless of genetic background. Several mechanisms could account for these effects in young control mice: 1) non-specific toxicity of MnTBAP in control mice, that is masked by the beneficial effects of ROS scavenging in obese UCP-DTA or db/db mice; 2) MnTBAP-facilitated proton leak through the inner mitochondrial membrane causing mitochondrial uncoupling in control mice; 3) scavenging of mitochondrial ROS below physiological levels in WT hearts. MnTBAP did not impair mitochondrial function in 24 week-old control mice. This discrepancy suggests that mitochondria from young mice are more susceptible to MnTBAP toxicity. Mitochondrial dysfunction and oxidative stress have previously been reported in the elderly relative to young subjects [31, 44], raising the possibility of increased oxidative stress in 24 week-old WT mice could have offset the ability of MnTBAP to scavenge ROS below physiological levels. Relative to 13-wk controls, 24-wk mice exhibited a nearly two fold increase in both fasting plasma insulin and triglyceride concentrations indicating insulin resistance, which could contribute to age-related mitochondrial dysfunction (Tables 1 and 2). Our study was not designed to directly compare mitochondrial energetics as a function of age, which would have required simultaneous analyses using similar stocks of reagents to prevent inter-assay variations.

Several groups have reported a correlation between mitochondrial dysfunction and insulin resistance [18, 44, 45]. Akt activation in response to insulin was not altered, but the glucose transport, glycolysis and glucose oxidation response to insulin were markedly blunted in UCP-DTA mice. Systemic administration of MnTBAP significantly improved the myocardial response to insulin in terms of glucose uptake, utilization, and ex vivo cardiac

function. Thus the normalization of glucose utilization by MnTBAP appeared to be largely independent of changes in proximal insulin signaling to Akt. GLUT4 translocation to the plasma membrane following insulin stimulation is the main mediator of insulin-stimulated glucose uptake by cardiomyocytes [46], although detailed molecular mechanism(s) remain incompletely understood [47]. In fact, decreased insulin-stimulated GLUT4 translocation, glucose uptake and utilization precede significant alterations in signaling molecules such as IRS, Akt and Akt substrate 160 (AS160) [48, 49]. Moreover, we recently reported that persistent PI3K signaling could impair cardiomyocyte glucose uptake despite normal GLUT4 translocation [50]. Future studies will investigate the molecular links between insulin-stimulated GLUT4 translocation, oxidative stress, and mitochondrial function in the heart.

Taken together, the present study reveals that obesity and insulin resistance is associated with mitochondrial dysfunction and oxidative stress in the heart. Our data suggest that even relatively low levels of long-term oxidative stress impairs the metabolic and functional response of the heart to insulin, independently of changes in the activation of proximal insulin signaling pathways. However, systemic administration of an antioxidant that mimics the mitochondrial enzyme SOD2 is sufficient to reverse mitochondrial dysfunction when administered at any stage in the progression of insulin resistance and diabetes. Although earlier administration may impact generalized insulin resistance, our data suggest that targeted anti-oxidants may improve myocardial mitochondrial function in more advanced stages of diabetes and obesity when effects on the systemic metabolic milieu were no longer observed. Thus directly targeting mitochondrial oxidative stress could represent an equally important therapeutic approach for ameliorating cardiac dysfunction, as are therapies that specifically target hyperglycemia and other systemic abnormalities associated with insulin resistance. ROS scavenging improves insulin-stimulated glucose transport and utilization in the hearts of mice with the metabolic syndrome, whilst having a deleterious impact in young control animals. Thus the use of antioxidant strategies in the context of obesity and insulin-resistant associated cardiac dysfunction might be most beneficial in those contexts when oxidative stress and mitochondrial dysfunction are central to the underlying pathophysiology.

5. Conclusions

Diabetes and obesity increase the risk of heart failure via multiple mechanisms including mitochondrial dysfunction, altered substrate metabolism and insulin insensitivity. The contribution of oxidative stress to these metabolic mechanisms is incompletely understood and whether or not these metabolic and signaling changes can be reversed by ROS scavenging is unknown. The present study shows that short term ROS scavenging normalizes mitochondrial energetics and insulin-stimulated glucose utilization, thereby providing additional mechanistic insights supporting the therapeutic utility of ROS scavenging as a therapy for obesity-related cardiomyopathy.

Supplementary Material

Refer to Web version on PubMed Central for supplementary material.

Acknowledgments

Sources of funding

This work was supported by grants RO1HL73167 and UO1HL70525 from the National Institutes of Health (NIH), and a research grant from the American Diabetes Association to E. Dale Abel who is an Established Investigator of the American Heart Association. OI was supported by T32DK091317 from the NIH, KMPP by the Coordenação de Aperfeiçoamento de Pessoal de Nível Superior (CAPES, Brazil) and HB by a postdoctoral fellowship of the German Research Foundation (DFG).

Glossary

AS160	ATP substrate of 160 Kilo Daltons
ATP	Adenosine triphosphate
CVD	Cardiovascular Disease
DEXA	Dual Energy X-ray Absorptiometry
GLUT4	Glucose Transporter 4
GSK3	Glycogen Synthase Kinase 3
IR	Insulin resistance
IRS	Insulin receptor substrate
MnSOD	Manganese superoxide dismutase
MnTBAP	Mn (III) tetrakis (4-benzoic acid) porphyrin Chloride
NDUFA	NADH dehydrogenase (ubiquinone), alpha
PI3K	Phosphoinositide 3-kinase
ROS	Reactive oxygen species
SOD2	Superoxide dismutase 2
UCP-DTA	Uncoupling protein 1 –Diphtheria Toxin A

References

1. Mente A, Yusuf S, Islam S, McQueen MJ, Tanomsup S, Onen CL, et al. Metabolic syndrome and risk of acute myocardial infarction a case-control study of 26,903 subjects from 52 countries. Journal of the American College of Cardiology. 2010; 55:2390–2398. [PubMed: 20488312]
2. Gerstein HC, Miller ME, Byington RP, Goff DC Jr, Bigger JT, et al. Action to Control Cardiovascular Risk in Diabetes Study G. Effects of intensive glucose lowering in type 2 diabetes. The New England journal of medicine. 2008; 358:2545–2559. [PubMed: 18539917]
3. Duckworth W, Abraira C, Moritz T, Reda D, Emanuele N, Reaven PD, et al. Glucose control and vascular complications in veterans with type 2 diabetes. The New England journal of medicine. 2009; 360:129–139. [PubMed: 19092145]
4. Boudina S, Sena S, O'Neill BT, Tathireddy P, Young ME, Abel ED. Reduced mitochondrial oxidative capacity and increased mitochondrial uncoupling impair myocardial energetics in obesity. Circulation. 2005; 112:2686–2695. [PubMed: 16246967]
5. Boudina S, Sena S, Theobald H, Sheng X, Wright JJ, Hu XX, et al. Mitochondrial energetics in the heart in obesity-related diabetes: direct evidence for increased uncoupled respiration and activation of uncoupling proteins. Diabetes. 2007; 56:2457–2466. [PubMed: 17623815]

6. Kuo TH, Moore KH, Giacomelli F, Wiener J. Defective oxidative metabolism of heart mitochondria from genetically diabetic mice. Diabetes. 1983; 32:781–787. [PubMed: 6414861]
7. Bugger H, Chen D, Riehle C, Soto J, Theobald HA, Hu XX, et al. Tissue-specific remodeling of the mitochondrial proteome in type 1 diabetic akita mice. Diabetes. 2009; 58:1986–1997. [PubMed: 19542201]
8. Li Y, Wende AR, Nunthakungwan O, Huang Y, Hu E, Jin H, et al. Cytosolic, but not mitochondrial, oxidative stress is a likely contributor to cardiac hypertrophy resulting from cardiac specific GLUT4 deletion in mice. The FEBS journal. 2012; 279:599–611. [PubMed: 22221582]
9. Hoehn KL, Salmon AB, Hohnen-Behrens C, Turner N, Hoy AJ, Maghzal GJ, et al. Insulin resistance is a cellular antioxidant defense mechanism. Proceedings of the National Academy of Sciences of the United States of America. 2009; 106:17787–17792. [PubMed: 19805130]
10. Houstis N, Rosen ED, Lander ES. Reactive oxygen species have a causal role in multiple forms of insulin resistance. Nature. 2006; 440:944–948. [PubMed: 16612386]
11. Duncan JG, Fong JL, Medeiros DM, Finck BN, Kelly DP. Insulin-resistant heart exhibits a mitochondrial biogenic response driven by the peroxisome proliferator-activated receptoralpha/PGC-1alpha gene regulatory pathway. Circulation. 2007; 115:909–917. [PubMed: 17261654]
12. Hamann A, Flier JS, Lowell BB. Decreased brown fat markedly enhances susceptibility to diet-induced obesity, diabetes, and hyperlipidemia. Endocrinology. 1996; 137:21–29. [PubMed: 8536614]
13. O'Connell KA, Dabkowski ER, de Fatima Galvao T, Xu W, Daneault C, de Rosiers C, et al. Dietary saturated fat and docosahexaenoic acid differentially effect cardiac mitochondrial phospholipid fatty acyl composition and Ca(2+) uptake, without altering permeability transition or left ventricular function. Physiological reports. 2013; 1:e00009. [PubMed: 24303101]
14. Galvao TF, Brown BH, Hecker PA, O'Connell KA, O'Shea KM, Sabbah HN, et al. High intake of saturated fat, but not polyunsaturated fat, improves survival in heart failure despite persistent mitochondrial defects. Cardiovascular research. 2012; 93:24–32. [PubMed: 21960686]
15. Chess DJ, Khairallah RJ, O'Shea KM, Xu W, Stanley WC. A high-fat diet increases adiposity but maintains mitochondrial oxidative enzymes without affecting development of heart failure with pressure overload. American journal of physiology Heart and circulatory physiology. 2009; 297:H1585–93. [PubMed: 19767529]
16. Day BJ, Fridovich I, Crapo JD. Manganic porphyrins possess catalase activity and protect endothelial cells against hydrogen peroxide-mediated injury. Archives of biochemistry and biophysics. 1997; 347:256–262. [PubMed: 9367533]
17. Day BJ, Shawen S, Liochev SI, Crapo JD. A metalloporphyrin superoxide dismutase mimetic protects against paraquat-induced endothelial cell injury, in vitro. The Journal of pharmacology and experimental therapeutics. 1995; 275:1227–1232. [PubMed: 8531085]
18. Boudina S, Bugger H, Sena S, O'Neill BT, Zaha VG, Ilkun O, et al. Contribution of impaired myocardial insulin signaling to mitochondrial dysfunction and oxidative stress in the heart. Circulation. 2009; 119:1272–1283. [PubMed: 19237663]
19. Schneider BD, Leibold EA. Effects of iron regulatory protein regulation on iron homeostasis during hypoxia. Blood. 2003; 102:3404–3411. [PubMed: 12855587]
20. Kim J, Wende AR, Sena S, Theobald HA, Soto J, Sloan C, et al. Insulin-like growth factor I receptor signaling is required for exercise-induced cardiac hypertrophy. Molecular endocrinology. 2008; 22:2531–2543. [PubMed: 18801929]
21. Bugger H, Riehle C, Jaishy B, Wende AR, Tuinei J, Chen D, et al. Genetic loss of insulin receptors worsens cardiac efficiency in diabetes. Journal of molecular and cellular cardiology. 2012; 52:1019–1026. [PubMed: 22342406]
22. Mazumder PK, O'Neill BT, Roberts MW, Buchanan J, Yun UJ, Cooksey RC, et al. Impaired cardiac efficiency and increased fatty acid oxidation in insulin-resistant ob/ob mouse hearts. Diabetes. 2004; 53:2366–2374. [PubMed: 15331547]
23. O'Neill BT, Kim J, Wende AR, Theobald HA, Tuinei J, Buchanan J, et al. A conserved role for phosphatidylinositol 3-kinase but not Akt signaling in mitochondrial adaptations that accompany physiological cardiac hypertrophy. Cell metabolism. 2007; 6:294–306. [PubMed: 17908558]

24. Riehle C, Wende AR, Sena S, Pires KM, Pereira RO, Zhu Y, et al. Insulin receptor substrate signaling suppresses neonatal autophagy in the heart. The Journal of clinical investigation. 2013; 123:5319–5333. [PubMed: 24177427]
25. Belke DD, Betuing S, Tuttle MJ, Graveleau C, Young ME, Pham M, et al. Insulin signaling coordinately regulates cardiac size, metabolism, and contractile protein isoform expression. The Journal of clinical investigation. 2002; 109:629–639. [PubMed: 11877471]
26. Frayn KN, Maycock PF. Skeletal muscle triacylglycerol in the rat: methods for sampling and measurement, and studies of biological variability. Journal of lipid research. 1980; 21:139–144. [PubMed: 7354251]
27. Wende AR, Soto J, Olsen CD, Pires KM, Schell JC, Larrieu-Lahargue F, et al. Loss of bradykinin signaling does not accelerate the development of cardiac dysfunction in type 1 diabetic akita mice. Endocrinology. 2010; 151:3536–3542. [PubMed: 20501666]
28. Mandarim-de-Lacerda CA. Stereological tools in biomedical research. Anais da Academia Brasileira de Ciencias. 2003; 75:469–486. [PubMed: 14605681]
29. Sena S, Rasmussen IR, Wende AR, McQueen AP, Theobald HA, Wilde N, et al. Cardiac hypertrophy caused by peroxisome proliferator- activated receptor-gamma agonist treatment occurs independently of changes in myocardial insulin signaling. Endocrinology. 2007; 148:6047–6053. [PubMed: 17823261]
30. Lowell BB, V SS, Hamann A, Lawitts JA, Himms-Hagen J, Boyer BB, et al. Development of obesity in transgenic mice after genetic ablation of brown adipose tissue. Nature. 1993; 366:740–742. [PubMed: 8264795]
31. Niemann B, Chen Y, Teschner M, Li L, Silber RE, Rohrbach S. Obesity induces signs of premature cardiac aging in younger patients: the role of mitochondria. Journal of the American College of Cardiology. 2011; 57:577–585. [PubMed: 21272749]
32. Shen X, Zheng S, Metreveli NS, Epstein PN. Protection of cardiac mitochondria by overexpression of MnSOD reduces diabetic cardiomyopathy. Diabetes. 2006; 55:798–805. [PubMed: 16505246]
33. Ye G, Metreveli NS, Donthi RV, Xia S, Xu M, Carlson EC, et al. Catalase protects cardiomyocyte function in models of type 1 and type 2 diabetes. Diabetes. 2004; 53:1336–1343. [PubMed: 15111504]
34. Boudina S, Sena S, Sloan C, Tebbi A, Han YH, O'Neill BT, et al. Early mitochondrial adaptations in skeletal muscle to diet-induced obesity are strain dependent and determine oxidative stress and energy expenditure but not insulin sensitivity. Endocrinology. 2012; 153:2677–2688. [PubMed: 22510273]
35. Pires KM, Ilkun O, Valente M, Boudina S. Treatment with a SOD mimetic reduces visceral adiposity, adipocyte death, and adipose tissue inflammation in high fat-fed mice. Obesity. 2014; 22:178–187. [PubMed: 23526686]
36. Bashan N, Kovsan J, Kachko I, Ovadia H, Rudich A. Positive and negative regulation of insulin signaling by reactive oxygen and nitrogen species. Physiological reviews. 2009; 89:27–71. [PubMed: 19126754]
37. Chiarugi P, Cirri P. Redox regulation of protein tyrosine phosphatases during receptor tyrosine kinase signal transduction. Trends in biochemical sciences. 2003; 28:509–514. [PubMed: 13678963]
38. Dai DF, Chen T, Szeto H, Nieves-Cintron M, Kutyavin V, Santana LF, et al. Mitochondrial targeted antioxidant Peptide ameliorates hypertensive cardiomyopathy. Journal of the American College of Cardiology. 2011; 58:73–82. [PubMed: 21620606]
39. Dai DF, Johnson SC, Villarin JJ, Chin MT, Nieves-Cintron M, Chen T, et al. Mitochondrial oxidative stress mediates angiotensin II-induced cardiac hypertrophy and Galphaq overexpression-induced heart failure. Circulation research. 2011; 108:837–846. [PubMed: 21311045]
40. Takimoto E, Kass DA. Role of oxidative stress in cardiac hypertrophy and remodeling. Hypertension. 2007; 49:241–248. [PubMed: 17190878]
41. St-Pierre J, Buckingham JA, Roebuck SJ, Brand MD. Topology of superoxide production from different sites in the mitochondrial electron transport chain. The Journal of biological chemistry. 2002; 277:44784–44790. [PubMed: 12237311]

42. Danielson SR, Held JM, Oo M, Riley R, Gibson BW, Andersen JK. Quantitative mapping of reversible mitochondrial Complex I cysteine oxidation in a Parkinson disease mouse model. The Journal of biological chemistry. 2011; 286:7601–7608. [PubMed: 21196577]
43. Lefort N, Glancy B, Bowen B, Willis WT, Bailowitz Z, De Filippis EA, et al. Increased reactive oxygen species production and lower abundance of complex I subunits and carnitine palmitoyltransferase 1B protein despite normal mitochondrial respiration in insulin-resistant human skeletal muscle. Diabetes. 2010; 59:2444–2452. [PubMed: 20682693]
44. Petersen KF, Befroy D, Dufour S, Dziura J, Ariyan C, Rothman DL, et al. Mitochondrial dysfunction in the elderly: possible role in insulin resistance. Science. 2003; 300:1140–1142. [PubMed: 12750520]
45. Wang CH, Wang CC, Wei YH. Mitochondrial dysfunction in insulin insensitivity: implication of mitochondrial role in type 2 diabetes. Annals of the New York Academy of Sciences. 2010; 1201:157–165. [PubMed: 20649552]
46. Huang S, Czech MP. The GLUT4 glucose transporter. Cell metabolism. 2007; 5:237–252. [PubMed: 17403369]
47. Larance M, Ramm G, James DE. The GLUT4 code. Molecular endocrinology. 2008; 22:226–233. [PubMed: 17717074]
48. Sloan C, Tuinei J, Nemetz K, Frandsen J, Soto J, Wride N, et al. Central leptin signaling is required to normalize myocardial fatty acid oxidation rates in caloric-restricted ob/ob mice. Diabetes. 2011; 60:1424–1434. [PubMed: 21441440]
49. Wright JJ, Kim J, Buchanan J, Boudina S, Sena S, Bakirtzi K, et al. Mechanisms for increased myocardial fatty acid utilization following short-term high-fat feeding. Cardiovascular research. 2009; 82:351–360. [PubMed: 19147655]
50. Zhu Y, Pereira RO, O'Neill BT, Riehle C, Ilkun O, Wende AR, et al. Cardiac PI3K-Akt impairs insulin-stimulated glucose uptake independent of mTORC1 and GLUT4 translocation. Molecular endocrinology. 2013; 27:172–184. [PubMed: 23204326]

Highlights

- Obesity impairs mitochondrial energetics and increases mitochondrial ROS in the heart
- These changes are associated with decreased insulin-mediated glucose utilization
- Treatment with a targeted antioxidant MnTBAP restores mitochondrial function and prevents ROS overproduction
- Antioxidant treatment normalizes myocardial insulin responsiveness
- These changes are independent of changes in systemic metabolic homeostasis

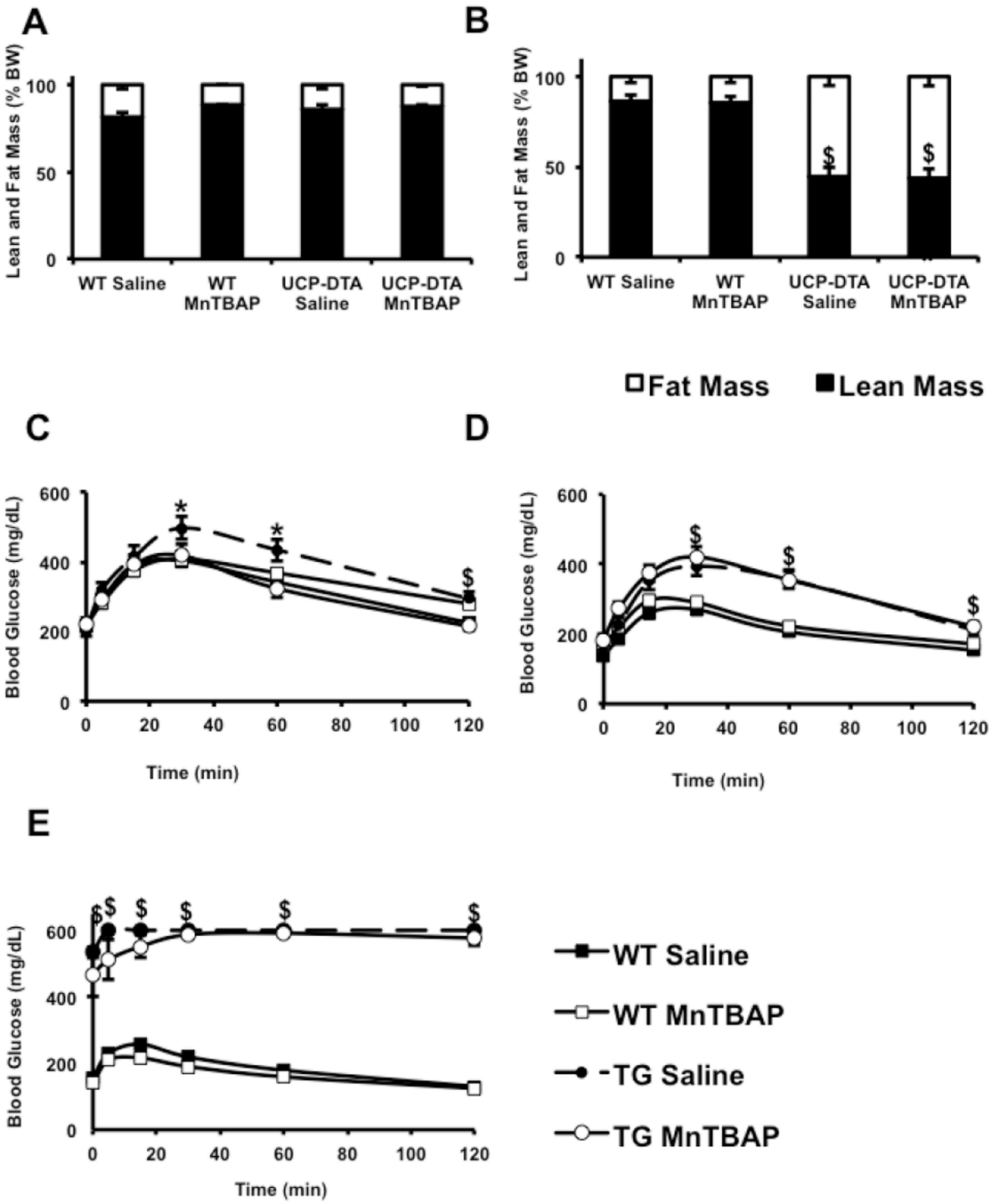

Figure 1. Impact of MnTBAP on body composition and glucose tolerance in UCP-DTA and db/db mice

A, B. Relative distribution of fat and lean mass as measured by DEXA in 13 and 24 week-old UCP-DTA mice vs. controls, respectively. Lean and fat mass is expressed as % of total body mass (n=3–9). **C–E.** Glucose tolerance tests in 13 week-old UCP-DTA, 24 week-old UCP-DTA, and 9 week-old db/db mice, respectively (n=6–15). Mice were treated with MnTBAP or saline, as indicated. Maximum glucose concentration detectable by the

glucometer is 600mg/dl. *p<0.05 vs. other genotypes; $ p<0.05 vs. WT saline and WT MnTBAP.

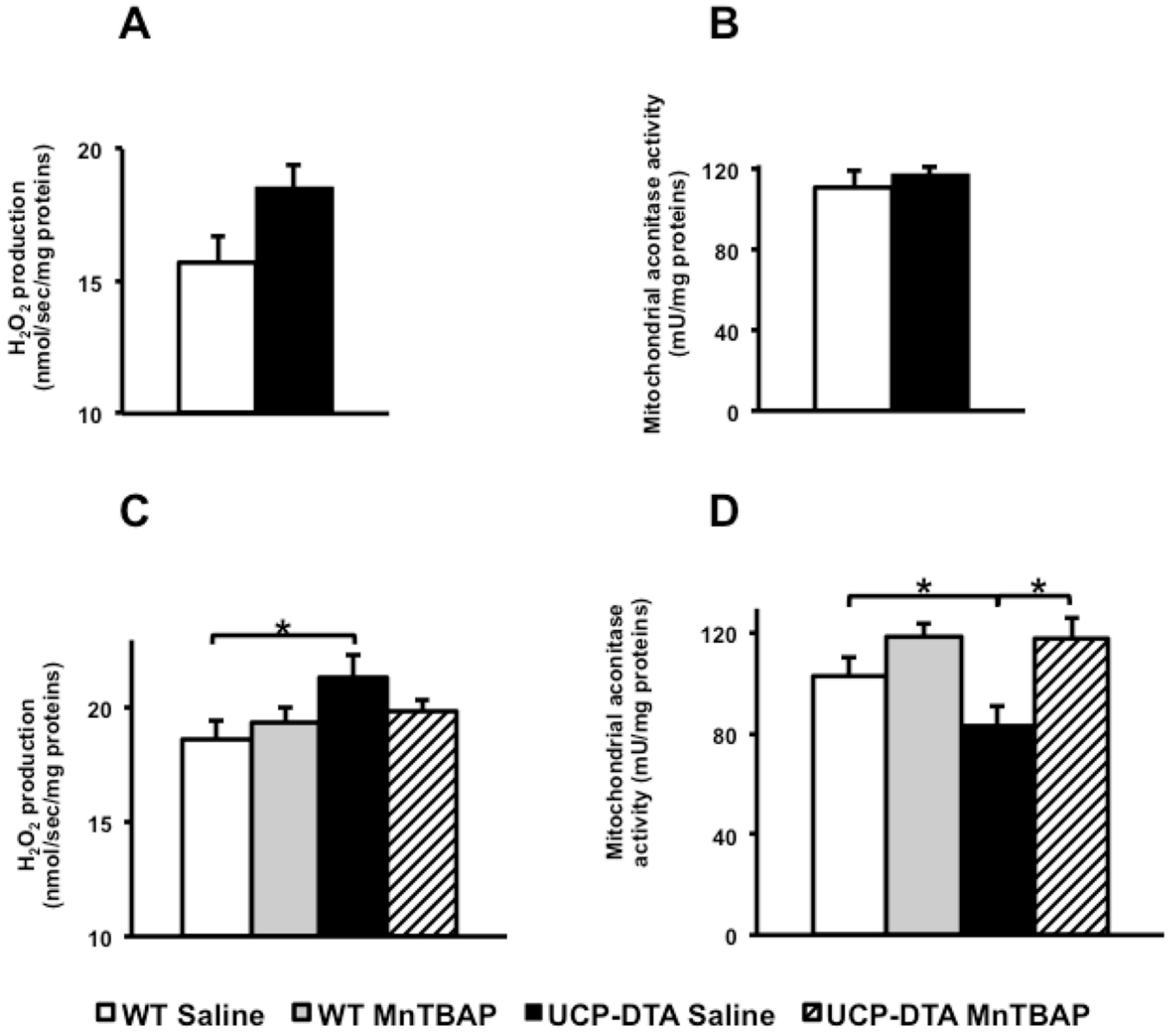

Figure 2. Evidence for mitochondrial oxidative stress and reversal by MnTBAP

A, B. No change in H_2O_2 emission and aconitase activity in 13 week-old UCP-DTA mice (n=3–4). **C.** The rate of H_2O_2 emission is increased in hearts of 24 week-old UCP-DTA mice treated with saline but not MnTBAP (n=6–7). **D.** Mitochondrial aconitase activity in hearts of 24 week-old UCP-DTA mice compared to WT littermates (n =4–6). *p<0.05 vs. all other or indicated groups.

□ Saline-treated control wildtype (WT) mice, ▨ MnTBAP-treated WT mice; ■ UCP-DTA treated with saline, ■ UCP-DTA treated with MnTBAP.

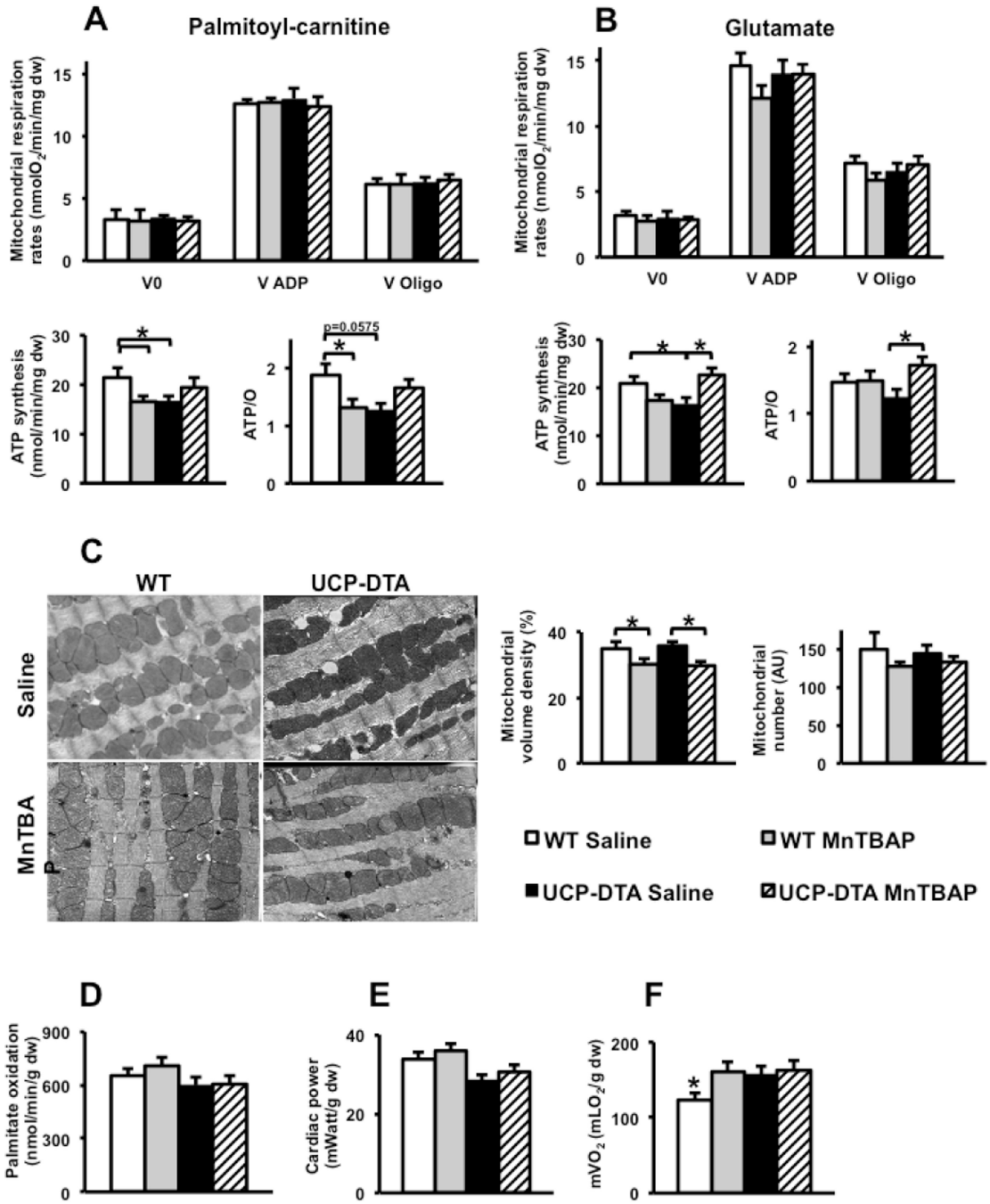

Figure 3. Impact of MnTBAP on mitochondrial function and myocardial substrate metabolism in 13 week-old UCP-DTA mice

A. Oxygen consumption, ATP synthesis, and ATP/O ratios measured using saponin-permeabilized LV fibers with palmitoyl-carnitine and malate as substrates (n =9–13). **B.** Oxygen consumption, ATP synthesis, and ATP/O ratios using saponin-permeabilized fibers with glutamate and malate as substrates (n=6–7). *p<0.05 vs. all or indicated groups. **C.** Electron microscopy (1:10,000) of left ventricular section in 13 week-old UCP-DTA mice, and quantification of mitochondrial volume density and number. n=4. **D–F.** Palmitate

oxidation, cardiac power and mVO_2 measured *ex vivo* in isolated working hearts (n=6). *p<0.05 vs. all other or indicated groups.

□ Saline-treated control wildtype (WT) mice, ▨ MnTBAP-treated WT mice, ■ UCP-DTA treated with saline, ■ UCP-DTA treated with MnTBAP. Dw=dry weight.

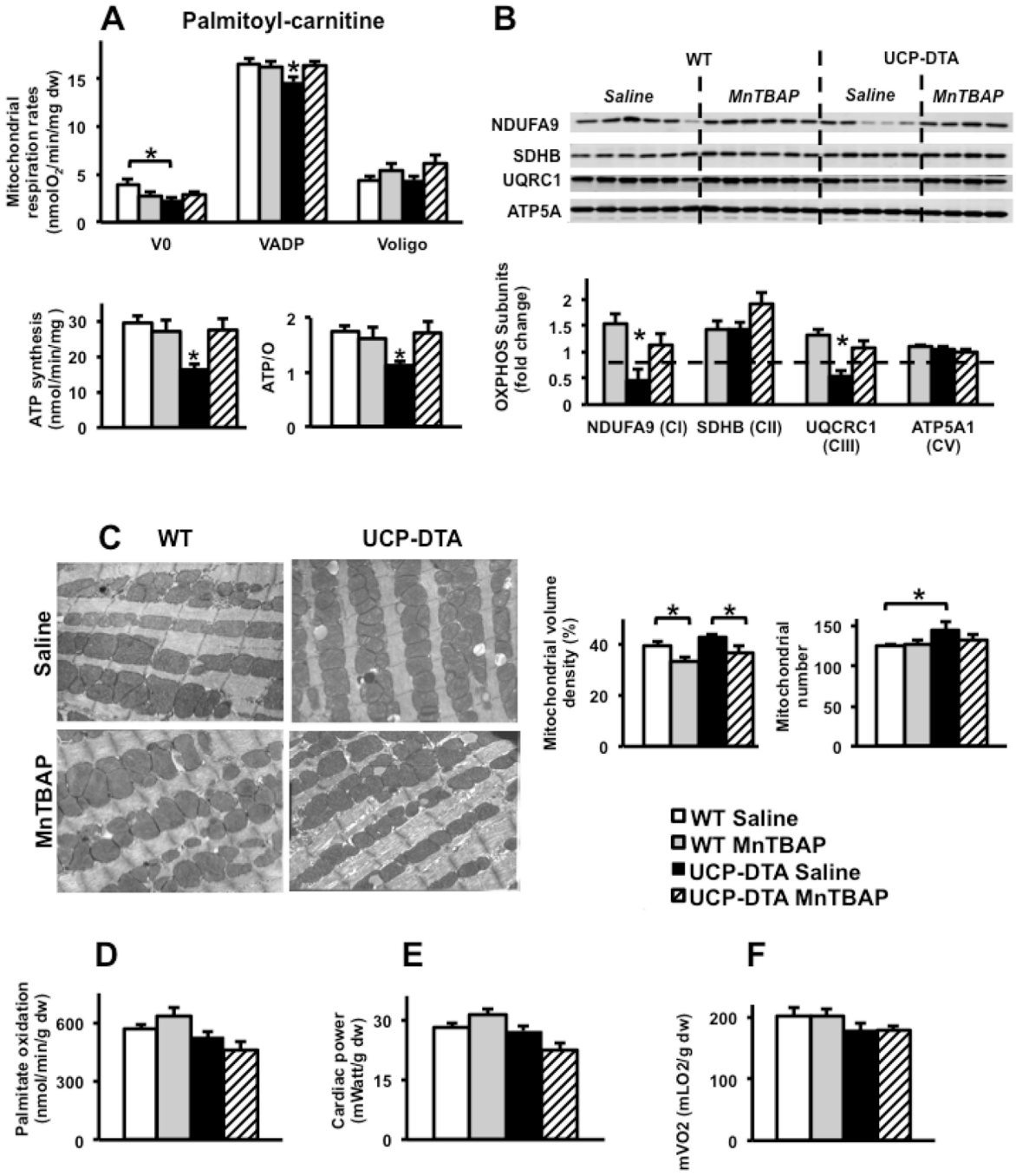

Figure 4. Impact of MnTBAP on mitochondrial function and myocardial substrate metabolism in 24 week-old UCP-DTA mice

A. Oxygen consumption, ATP synthesis, and ATP/O ratios measured using saponin-permeabilized LV fibers with palmitoyl-carnitine and malate as substrates (n=6–8). **B.** Abundance and densitometric analysis of selected OxPhos subunits in the whole heart homogenates as measured by western blotting (n=4–6). **C.** Electron microscopy images (1:10,000) and quantification of mitochondrial number and volume density in left ventricular sections of 24 week-old UCP-DTA mouse hearts (n=4). **D–F.** Palmitate

oxidation, cardiac power and mVO_2 measured *ex vivo* in isolated working hearts (n=6–8). *p<0.05 vs. all other or indicated groups.

Dashed line or □ Saline-treated control wildtype (WT) mice, ▨ MnTBAP-treated WT mice, ■ UCP-DTA treated with saline, ■ UCP-DTA treated with MnTBAP. Dw=dry weight.

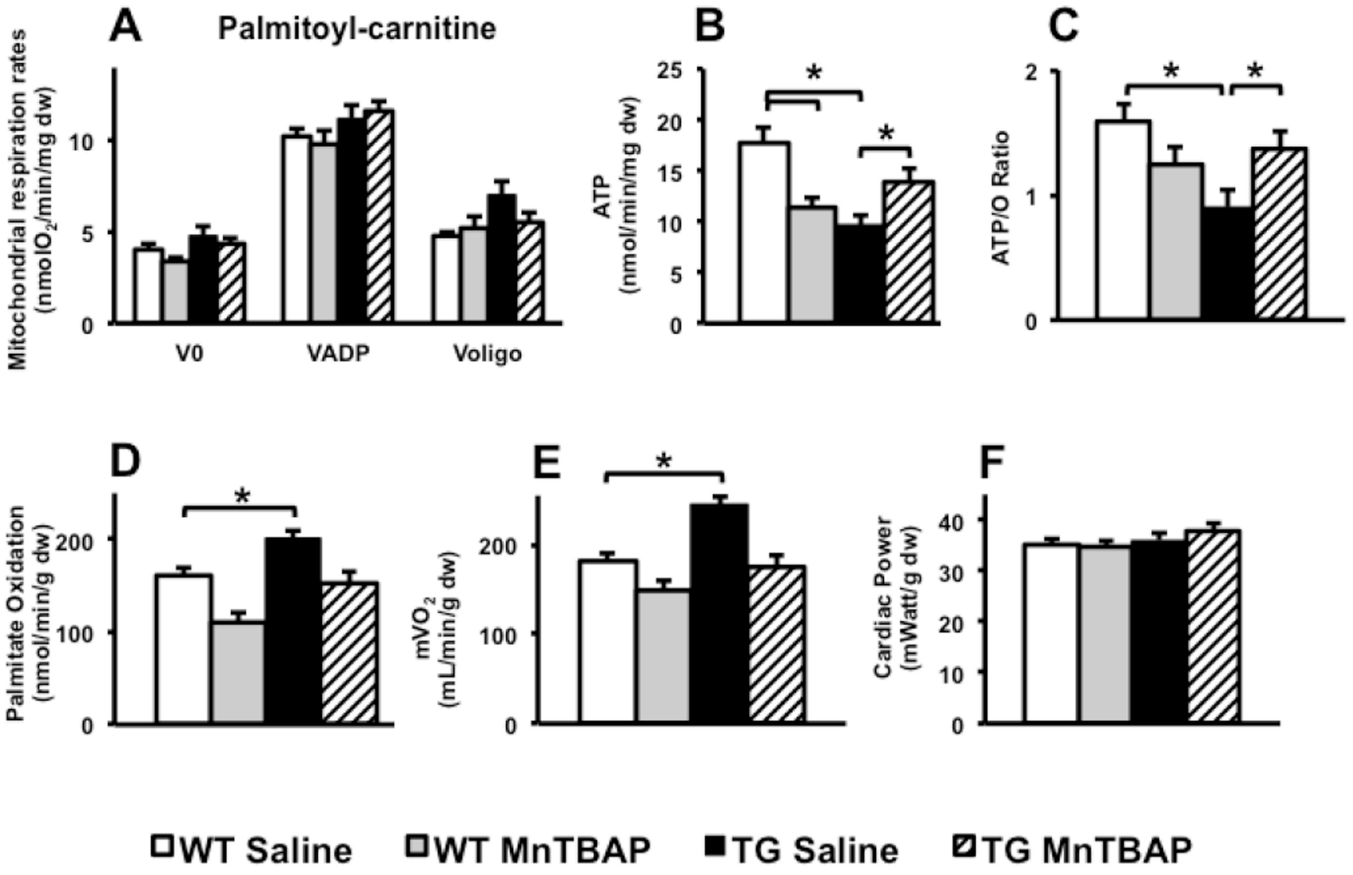

Figure 5. Impact of MnTBAP on mitochondrial function and myocardial substrate metabolism in 9 week-old db/db mice

A–C. Oxygen consumption, ATP synthesis, and ATP/O ratios measured using saponin-permeabilized LV fibers with palmitoyl-carnitine and malate as substrates (n=6–8). **D–F.** Palmitate oxidation, cardiac power and mVO_2 measured *ex vivo* in isolated working hearts (n=4–5). *p<0.05 vs. all other or indicated groups.

□ Saline-treated control wildtype (WT) mice, ▨ MnTBAP-treated WT mice, ■ db/db treated with saline, ▩ db/db treated with MnTBAP. Dw=dry weight.

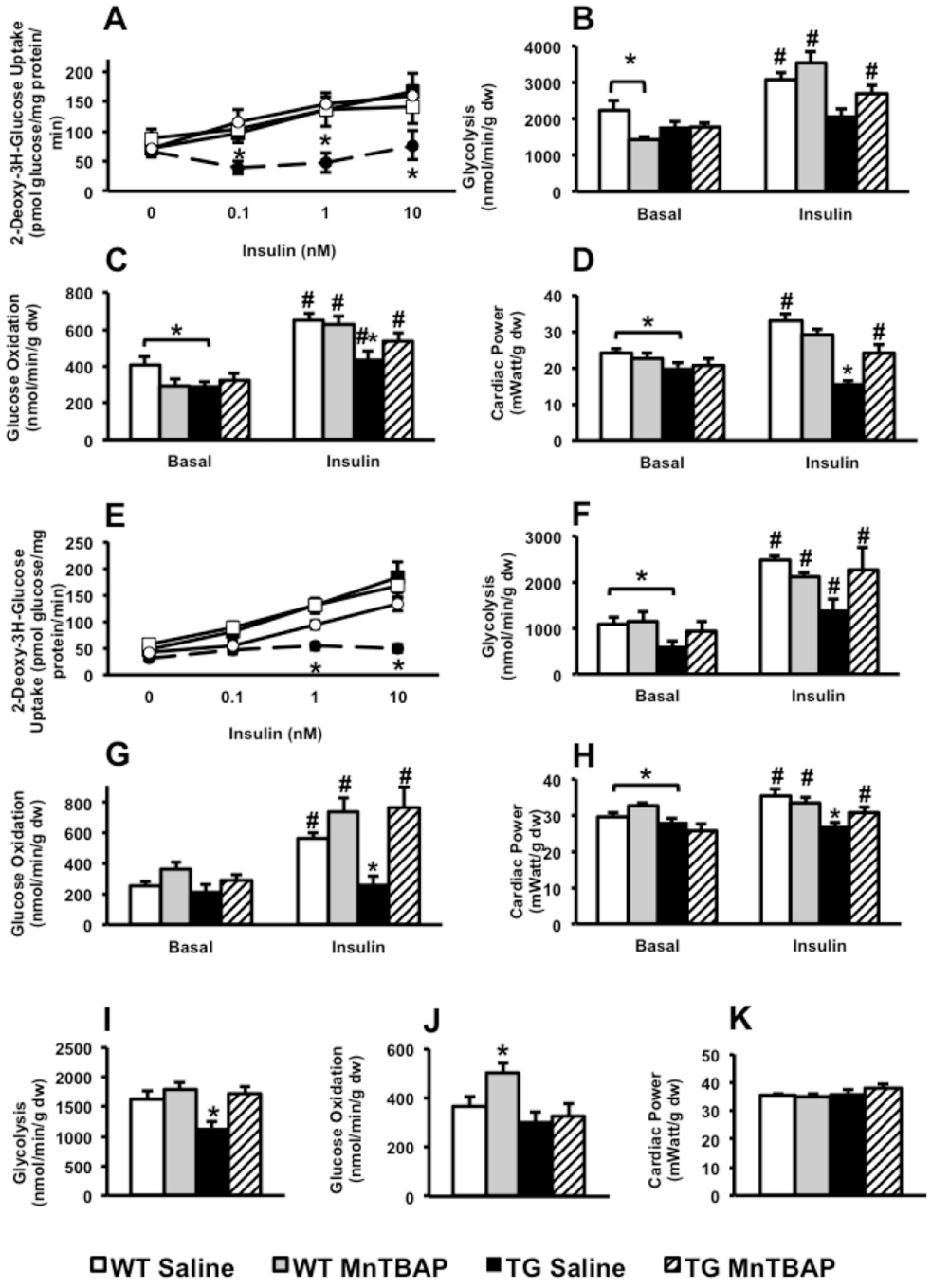

Figure 6. Impact of MnTBAP on insulin-stimulated cardiomyocyte glucose uptake and myocardial glucose utilization in 13 and 24-week-old UCP-DTA mice

A. Insulin-stimulated 2-deoxy-^{3}H-glucose uptake in isolated cardiomyocytes from 13 week-old and control hearts treated with saline or MnTBAP (n=4–5). **B–D.** Glycolysis, glucose oxidation, and cardiac power measured in isolated working heart preparations with or without 1nM insulin in 13 week-old UCP-DTA and control mice (n=5–7). **E.** Insulin-stimulated 2-deoxy-^{3}H-glucose uptake in isolated cardiomyocytes from 24 week-old UCP-DTA and control hearts treated with saline or MnTBAP (n=5–7). **F–H.** Glycolysis, glucose

oxidation, and cardiac power measured in isolated working heart preparations with or without 1nM insulin in 24 week-old UCP-DTA or control mice (n=5–7). **I–K.** Glycolysis, glucose oxidation, and cardiac power in db/db hearts measured in isolated working heart preparations without insulin (n=3–4). *p<0.05 vs. other genotypes in the same treatment group; # p<0.05 for insulin- stimulated vs. basal state for same genotype.
□ Saline-treated control wildtype (WT) mice, ▨ MnTBAP-treated WT mice, ■ UCP-DTA or db/db mice treated with saline, ■ UCP-DTA or db/db mice, treated with MnTBAP. Dw=dry weight.

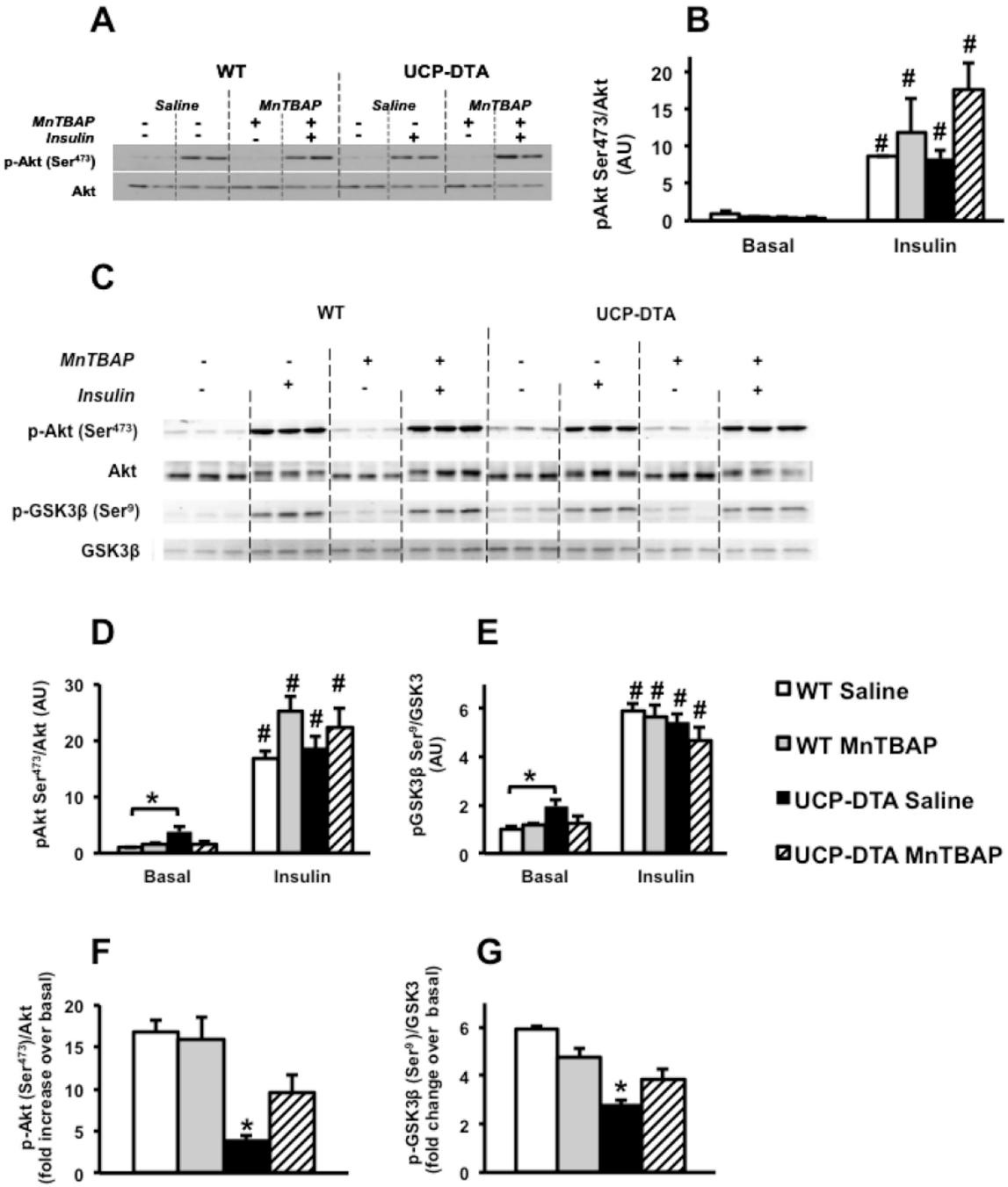

Figure 7. Insulin signaling in hearts of 13 or 24 week-old UCP-DTA and control mice treated with saline or MnTBAP

A, B. Western blots and densitometric analysis representing phosphorylation of Akt in 13 week-old UCP-DTA and control hearts perfused with or without 1nM insulin (n=4). **C–E.** Western blots and densitometric analysis representing phosphorylation of Akt and GSK3 in 24 week-old UCP-DTA and control hearts with or without 1nM insulin. **E, F.** Fold increase of insulin stimulated phospho-Akt and GSK3 over basal (n=5). *p<0.05 vs. other genotypes in the same groups; # p<0.05 for insulin- stimulated vs. basal state for same genotype.

□ Saline-treated control wildtype (WT) mice, ▨ MnTBAP-treated WT mice, ■ UCP-DTA treated with saline, ■ UCP-DTA treated with MnTBAP.

Table 1

Characteristics of 13 week-old UCP-DTA (UD) mice.

	WT Saline	WT MnTBAP	UD Saline	UD MnTBAP
n	8	7	8	7
Body Weight (g)	30.57 ± 0.62	30.08 ± 0.59	33.36 ± 1.03	34.05 ± 1.57
Heart Weight (mg)	128.0 ± 3.1	128.8 ± 2.7	139.2 ± 3.2	142.1 ± 4.6
HW/TL (mg/mm)	7.7 ± 0.2	7.4 ± 0.2	8.2 ± 0.2	8.2 ± 0.2
Glucose (mg/dL)	215.0 ± 15	216.1 ± 13.7	201.6 ± 12.6	221 ± 19.3
Insulin (ng/mL)	0.300 ± 0.023	0.366 ± 0.043	0.806 ± 0.183 $	0.818 ± 0.263 $
Triglycerides (mM)	2.112 ± 0.260	1.690 ± 0.326	3.748 ± 0.500 $	3.113 ± 0.532

$ $p<0.05$ vs. WT saline and WT MnTBAP.

HW, heart weight; TL, tibia length. Metabolites were measured after a 6-hr fast.

Table 2

Characteristics of 24 week-old UCP-DTA (UD) mice.

	WT Saline	WT MnTBAP	UD Saline	UD MnTBAP
n	15	15	15	15
Body Weight (g)	31.94 ± 0.7	32.28 ± 0.6	49.56 ± 1.1 $	47.87 ± 0.9 $
Heart Weight (mg)	121.0 ± 2.6	118.7 ± 2.7	163.0 ± 5.1&$	151.2 ± 2.6 $
HW/TL (mg/mm)	6.8 ± 0.15	6.7 ± 0.16	9.2 ± 0.27&$	8.5 ± 0.17 $
Glucose (mg/dL)	137.8 ± 4.0	159.1 ± 7.2	149.8 ± 12.6	183.3 ± 15.7
Insulin (ng/mL)	0.60± 0.11	0.49 ± 0.03	3.29 ± 0.34 $	3.34 ± 0.45 $
Triglycerides (mM)	3.83 ± 0.38	3.55 ± 0.36	5.39 ± 0.485 $	5.17 ± 0.59 $

$ $p<0.05$ vs. WT saline and WT MnTBAP.

& $p<0.05$ vs. UD (UCP-DTA) MnTBAP.

Metabolites were measured after a 6-hr fast.

Table 3

Characteristics of 9 week-old db/db mice.

	WT Saline	WT MnTBAP	db/db Saline	db/db MnTBAP
n	4	4	4	4
Body Weight (g)	22.31 ± 1.1	21.84 ± 0.4	40.06 ± 0.9 $	36.86 ± 1.5 $
Heart Weight (mg)	152 ± 11.4	132.25 ± 6.5	135.25 ± 6.1	133 ± 14.2
Glucose (mg/dL)	157.67 ± 9.6	139.67± 7.0	534.17 ± 16.4 $	467.83± 68.4 $
Insulin (ng/mL)	0.291± 0.031	0.254 ± 0.040	2.157± 0.282 $	2.367 ± 0.513 $
Triglycerides (mM)	0.686 ± 0.06*	1.47 ± 0.24	1.94 ± 0.34*	1.4 ± 0.15
Triglycerides-Fed	3.93 ± 0.66	5.46 ± 0.69	16.10 ± 0.86*	6.49 ± 0.29

$ p<0.05 vs. WT saline and WT MnTBAP,

* p<0.05 vs. all other groups.

Metabolites were measured after a 6-hr fast, unless indicated.

Table 4

Cardiac dimensions and function measured in 24 week-old UCP-DTA (UD) mice by echocardiography.

	WT Saline	WT MnTBAP	UD Saline	UD MnTBAP
n	6	7	7	6
IVSd (cm)	0.092 ± 0.006	0.091 ± 0.004	0.111 ± 0.003 $	0.106 ± 0.002 $
IVSs (cm)	0.131 ± 0.006	0.131 ± 0.007	0.155 ± 0.003 $	0.144 ± 0.003
LVIDd (cm)	0.378 ± 0.007	0.377 ± 0.011	0.412 ± 0.010 $	0.400 ± 0.018
LVIDs (cm)	0.278 ± 0.008	0.270 ± 0.011	0.307 ± 0.010 $	0.289 ± 0.018
LVPWd (cm)	0.09 ± 0.005	0.084 ± 0.005	0.093 ± 0.006	0.090 ± 0.007
LVPWs (cm)	0.112 ± 0.006	0.102 ± 0.005	0.109 ± 0.007	0.105 ± 0.006
EF (%)	60.53 ± 1.43	63.23 ± 1.81	58.74 ± 1.36	62.20 ± 2.58
FS (%)	26.7 ± 0.9	28.48 ± 1.19	25.61 ± 0.82	27.87 ± 1.6
HR (beats/min)	531.5 ± 28.6	518.1 ± 17.37	544.19 ± 9.20	557.64 ± 18.55
SV (mL)	0.036 ± 0.001	0.035 ± 0.003	0.041 ± 0.003	0.039 ± 0.004

$ $p<0.05$ vs. WT saline and WT MnTBAP

IVSd, interventricular septum thickness in diastole; IVSs, interventricular septum thickness in systole; LVIDd, left-ventricular internal diameter in diastole; LVDs, left-ventricular internal diameter in systole; LVPWd, left-ventricular posterior wall thickness in diastole; LVPWs, left-ventricular posterior wall thickness in systole; EF, ejection fraction; FS, fractional shortening; HR, heart rate; SV, stroke volume